Electron Transport Analysis for Improvement of Solid-State Dye-Sensitized Solar Cells Using Poly(3,4-ethylenedioxythiophene) as Hole Conductors†

Norihiro Fukuri, Naruhiko Masaki, Takayuki Kitamura, Yuji Wada, and Shozo Yanagida*

Material and Life Science, Graduate School of Engineering, and Center for Advanced Science and Innovation, Osaka University, Suita, Osaka 565-0871, Japan

Received: July 13, 2006; In Final Form: September 7, 2006

Dye-sensitized solar cells (DSCs) using solid-state hole conductor, poly(3,4-ethylenedioxythiophene) (PEDOT), were fabricated using in-situ photoelectrochemical polymerization giving short-circuit photocurrent density of 3.20 mA cm^{-2}, open-circuit voltage of 0.77 V, and fill factor of 0.50, and the resulting overall conversion efficiency of 1.25% on average under air mass 1.5 conditions. Furthermore, the electron transport properties of the DSCs based on PEDOT (PEDOT/DSCs) were analyzed using light intensity modulation induced photocurrent and photovoltage decay (SLIM-PCV) measurements and electrochemical impedance spectroscopy (EIS) measurements, and then compared to those of the DSCs based on organic liquid electrolyte containing I^-/I_3^- as redox couple (liquid iodide/iodine electrolyte-DSCs, iodide/DSCs for short). The effective filling of PEDOT in the mesopores of dyed TiO_2 layers is an important key to achieve the respectable conversion efficiency of PEDOT/DSCs that is comparable with iodide/DSCs.

Introduction

Dye-sensitized solar cells (DSCs) composed of mesoporous TiO_2 layers as electron conductor, ruthenium complex dyes as sensitizers, and liquid electrolyte containing I^-/I_3^- redox couple as a hole conductor have been under intensive research for the past decade due to high conversion efficiency (∼11%), simple fabrication process, and low production cost.[1−4] During the photoillumination to DSCs, photoexcited electrons by dye sensitization are rapidly injected into the conduction band of TiO_2 and diffuse in TiO_2 layers with the aid of a long-lifetime electron.[5,6] The I^-/I_3^- redox couple in the electrolyte reduces the oxidized dye and transports hole carriers to the counter electrode. In this system, the employment of both the TiO_2 having a large surface area available for dye adsorption and the fluid liquid electrolyte containing a redox species that is easy to immerse in mesoporous TiO_2 layers enables us to generate high photocurrent density up to ∼20 mA cm^{-2}.[7] However, the fault of DSCs using organic liquid electrolyte (liquid iodide/iodine electrolyte-DSCs, iodide/DSCs for short) is poor long-term stability due to leakage of electrolyte and sublimation of iodine.[8] To solve these problems, many attempts have been made to substitute the liquid electrolytes by other solid materials. Quasi-solid-state DSCs using polymeric or monomeric gel materials incorporated with I^-/I_3^- as redox couple,[9−11] polymer electrolyte,[12] or solid-state DSCs using p-type inorganic semiconductors,[13−15] or organic hole conductor[16−19] were investigated.

An organic hole conducting polymer, poly(3,4-ethylenedioxythiophene) (PEDOT), has higher hole mobility, stability, and transparency in the visible-light region compared to the other hole conducting polymers.[20−23] Figure 1 shows the chemical structure of PEDOT, which has a cis−trans π-conjugated backbone. When PEDOT is oxidized from a neutral state to an oxidized one, its electrical conductivity, stability, and optical properties are drastically changed. Due to such unique electrical properties and high stability, PEDOT is one of the most promising organic semiconductive polymers and is utilized in industrial applications.[20−23] In addition, we previously revealed that PEDOT can be used as a catalyst similar to Pt at a counter electrode.[24] We recently reported the application of in-situ photoelectrochemical polymerization of 3,4-ethylenedioxythiophene dimer (bis-EDOT) to construct solid-state DSCs based on PEDOT (PEDOT/DSCs), which gave a short-circuit photocurrent density (J_{sc}) of 2.3 mA cm^{-2}, an open-circuit voltage (V_{oc}) of ∼0.5 V, a fill factor (FF) of 0.5, and the conversion efficiency (η) of 0.53%.[25,26] However, the cell performance using in-situ photo-electrochemically polymerized PEDOT was still much lower than the cell using liquid electrolyte containing the I^-/I_3^- redox couple. In addition, the direct contact of PEDOT with either conducting glass anode or mesoporous TiO_2 surface induces short-circuit and back-electron transfer, resulting in a decrease of the cell performance. To prevent the back-electron transfer, i.e., improvement of shunt resistance, we reported employment of both the amphiphilic ruthenium dye with long alkyl chain, *cis*-RuLL′$(SCN)_2$ (L = 4,4′-dicarboxylic acid-2,2′-bipyridine, L′ = 4,4′-dinonyl-2,2′-bipyridine) (Z907 dye), and the nanocrystalline TiO_2 film anode on which the surface is treated with $Al(O^iBu)_3$, yielding the devices using PEDOT with enhancement of J_{sc}, V_{oc}, and FF, and the resulting η was achieved to 0.93%.[27]

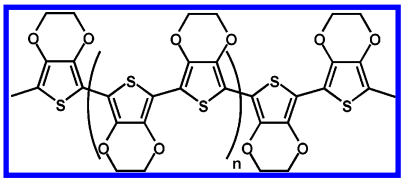

Figure 1. Chemical structure of poly(3,4-ethylenedioxythiophene) (PEDOT).

Since the electron transport processes play a decisive role at interfaces between mesoporous materials, dye molecules, and hole transport materials, it is essential to clarify the problem of the interface in function, optimizing PEDOT/DSCs with re-

† Part of the special issue "Arthur J. Nozik Festschrift".

10.1021/jp064439a CCC: $33.50
Published on Web 10/12/2006

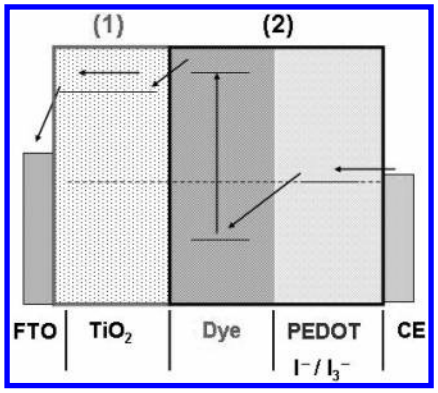

Figure 2. Schematic view of electron transport processes in DSCs.

spectable conversion efficiency. The electron transport processes in DSCs can be divided into the following two parts, as shown in Figure 2. Namely, the first one is the transport of injected electrons in the mesoporous TiO_2 layer, and the second concerns the charge transport in the hole conducting layer, including both liquid electrolyte containing I^-/I_3^- and PEDOT. The electron transport and electron lifetime in TiO_2 electrodes filled with liquid electrolyte has been already studied by intensity modulated photocurrent spectroscopy (IMPS),[28−30] pulsed laser-induced current transients,[31] intensity modulated photovoltage spectroscopy (IMVS),[32] and open-circuit photovoltage decay (OCVD).[33] It is clarified that electrons diffuse through the mesoporous TiO_2 layer and their diffusion is promoted by cationic species on the TiO_2, which is called ambipolar diffusion.[34,35] We previously reported the enhancement of the electron diffusion coefficient by increasing the concentration of cationic species in the liquid electrolyte.[10,34,35] Furthermore, the diffusing electrons in the mesoporous TiO_2 layer may be captured by either oxidized dye molecules or I_3^- as oxidizers in DSCs, which process reduces the lifetime of the electron in unidirectional electron flow.[15,36−39] Until now, several works on both the electron diffusion coefficient in TiO_2 electrodes and the electron lifetime of solid-state DSCs have been reported.[15,39] In those papers, the electron lifetime of solid-state DSCs based on p-type inorganic semiconductor, CuSCN, or organic hole conductor, spiro-MeOTAD [2,2′-7,7′-tetrakis(*N*,*N*-di-*p*-methoxyphenylamine)-9,9′-spirobifluorene], was estimated by photovoltage transient or IMVS, showing shorter electron lifetime than that of iodide/DSCs. To analyze the interfacial charge-transfer resistances and the electrochemical capacitances formed between dyed TiO_2 electrodes and electrolyte interfaces in DSCs, electrochemical impedance spectroscopy (EIS) was utilized.[40−44] The EIS measurement has been an effective method to obtain the information about the improvement of the performance of the cell by analyzing equivalent circuits of the DSCs. The Cole−Cole plots and Bode plots let us image how the *RC* circuits exist inside the DSCs and the frequency dependences of the cells, respectively.

In this work, we analyzed the electron transport processes in TiO_2 electrodes using stepped light induced transient measurements of photocurrent and voltage (SLIM-PCV).[45] The processes at TiO_2•dye/hole conductor and hole conductor/counter electrode interfaces in PEDOT/DSCs were evaluated on the basis of EIS measurements. The comparison with those values of PEDOT/DSCs and iodide/DSCs led us to successful clarification of the relative differences. In addition, we focused on an improvement of the polymerization conditions of bis-EDOT under Xe lamp illumination in order to construct good contacts between the hole conductor, PEDOT, and the counter electrode.

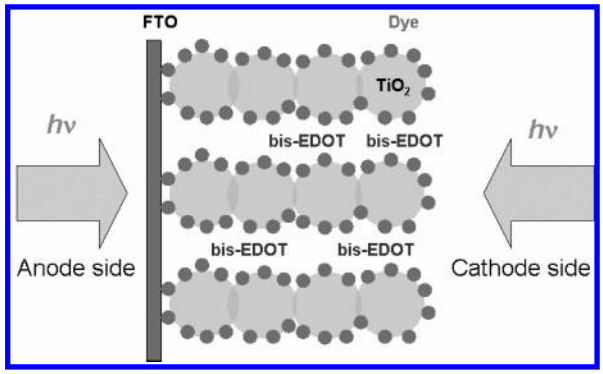

Figure 3. Graphic illustration of light illumination direction in in-situ photo-electrochemical polymerization of bis-EDOT.

Experimental Section

Preparation of PEDOT/DSCs and Iodide/DSCs. Thin compact TiO_2 layers were deposited by spin coating of Ti(O^i-Pr)$_4$ (Wako) in ethanol solution on conducting fluorine-doped SnO_2 glass substrates (FTO, 10 Ω square^{-1}, Nippon Sheet Glass) in order to prevent the direct contacts between FTO and PEDOT through the void inevitably formed between FTO and mesoporous TiO_2 layers.[26,27] Then, mesoporous TiO_2 layers that have different thicknesses of 2−5 μm were prepared on the compact TiO_2-layered FTO substrates using a TiO_2 paste (Nanoxide-T, Solaronix) by doctor blade technique and sintered at 500 °C for 1 h. The thickness of TiO_2 layer was measured using a surface profiler (Dektak 3, Sloan). The sintered TiO_2 electrodes were immersed in a 5.0×10^{-4} M amphiphilic ruthenium dye, *cis*-RuLL′(SCN)$_2$ (L = 4,4′-dicarboxylic acid-2,2′-bipyridine, L′ = 4,4′-dinonyl-2,2′-bipyridine) (Z907, Ruthenium 520-DN, Solaronix), acetonitrile/*tert*-butyl alcohol = 1:1 solution for 24 h to adsorb Z907 dye, and then rinsed with acetonitrile. The typical amount of adsorbed Z907 on TiO_2 was ca. 7.6×10^{-8} mol/cm^3 evaluated from the absorptiometry.

PEDOT was introduced into the mesopores of the Z907-adsorbed TiO_2 layers using in-situ photo-electrochemical polymerization of bis-EDOT.[26,27] Bis-EDOT was synthesized according to a reported method.[46] A three-electrode cell with a dyed TiO_2 working electrode, a Pt wire counter electrode, and an Ag/AgCl reference electrode filled with 0.1 M $LiClO_4$, $NaClO_4$, or (TBA)ClO_4 (TBA = tetrabutylammonium; Wako) acetonitrile solution containing 0.01 M bis-EDOT was employed under potentiostatic conditions. The potential of +0.20 V vs Ag/AgCl was applied to the dyed TiO_2 electrode under the illumination of a 500 W Xe lamp (λ > 520 nm, 18 mW cm^{-2}) for 15−30 min. The photo-electrochemical polymerization of bis-EDOT was performed from either FTO/TiO_2-side (anode-side) illumination or counter electrode combination-side (cathode-side) illumination by Xe lamp. Figure 3 shows the graphic illustration of Xe lamp illumination direction.

After the polymerization, TiO_2/dye/PEDOT electrodes were dried at room temperature and then treated with an ionic liquid, 1-ethyl-3-methylimidazolium bis(trifluoromethylsulfonyl)imide (EMImTFSI) containing 0.2 M LiTFSI and 0.2 M 4-*tert*-butylpyridine (*t*BP) for 24 h as described elsewhere.[26,27] In the case of TiO_2/dye/PEDOT electrodes which are polymerized using $NaClO_4$ or (TBA)ClO_4 instead of $LiClO_4$, the electrodes were treated with EMImTFSI containing only 0.2 M *t*BP in order to clarify the effect of Li^+ cations. After the fabrication of TiO_2/dye/PEDOT electrodes, the working electrodes were clipped with Au-sputtered counter electrodes (surface resistance, 2−3 Ω) to fabricate the sandwich-type photovoltaic cells.

TABLE 1: Polymerization Charge and the Cell Performance of PEDOT/DSCs

	polymerization charge (mC cm^{-2})	J_{sc} (mA cm^{-2})	V_{oc} (V)	FF	η (%)	η_{max} (%)
anode side[a]	20.8 ± 3.9	2.76 ± 0.42	0.66 ± 0.07	0.36 ± 0.02	0.64 ± 0.05	0.67
cathode side[b]	15.2 ± 1.9	3.20 ± 0.27	0.77 ± 0.02	0.50 ± 0.12	1.25 ± 0.38	2.09

[a] Average of 3 samples. [b] Average of 6 samples

On the other hand, the iodide/DSCs were fabricated using the following electrolyte solution: 0.6 M 1,2-dimethyl-3-propylimidazolium iodide (DMPImI: Shikoku Corp.), 0.05 M I_2, 0.1 M LiI, and 0.5 M *t*BP in methoxyacetonitrile. After preparing that, the Z907-dyed TiO_2 electrodes were connected with a Pt-sputtered counter electrode (surface resistance, 16−18 Ω) by thermal adhesive sealant (HIMILAN 1652, Mitsui-Dupont Polychemical; thickness = 50 μm), and then the electrolyte solution was injected from the hole on the back of the Pt counter electrode to the dyed TiO_2 electrode area. Finally, the hole was covered with a cover glass (Iwaki glass) to fabricate the sealed-type iodide/DSCs. The area of fabricated cells was about 0.15 cm^2.

Measurements. The polymerization currents were measured using a BAS-100 B/W under potentiostatic conditions. The total charges during polymerization reactions were calculated by integration of polymerization currents and referred to as polymerization charges. Since polymerization currents include the contributions of diffusion of ionic species and doping of anions into PEDOT, polymerization charges are corresponding to the ideal maximum amounts of polymerized EDOT, e.g. 5.2 × 10^{-7} mol cm^{-2} at 25 mC cm^{-2}.

The photoenergy conversion efficiency of fabricated DSCs was obtained using a PC controlled voltage−current source meter (R6246, Advantest) under a solar simulator illumination (Yamashita Denso, YSS-80) of air mass 1.5 (100 mW cm^{-2}) conditions at 25 °C. The incident photon to current conversion efficiency (IPCE) was measured using a commercial setup for IPCE measurements (PV-25DYE, JASCO) under 5 mW cm^{-2} monochromic light illumination. The measured IPCE values take into account the incident light loss due to the absorption and reflection by FTO glass.

The electron diffusion coefficient in mesoporous TiO_2 electrodes of both PEDOT/DSCs and iodide/DSCs was measured by stepped light induced transient measurements of photocurrent and voltage as described elsewhere.[45] The short-circuit photocurrent decay was obtained by slight step modulation of the illumination intensity of a diode laser (Lablasers, Coherent, λ = 635 nm) by a function generator (Toho Technical Research, FG-02), then amplified by a current amplifier (Sanford Research Systems, SR570), and monitored by an oscilloscope (Tektronix TDS3052). In the same way, the electron lifetimes of both PEDOT/DSCs and iodide/DSCs were determined from transient measurements of photovoltage under the open-circuit conditions using the laser. The open-circuit photovoltage decay was amplified by a differential amplifier (5307, NF Electronic Instruments) and monitored by the oscilloscope. In both measurements, the laser irradiation was performed in the direction toward the anode of the cells and its intensity was controlled using neutral density filters. The theory and setup of those measurements are also described in the literature.[45]

The EIS of both PEDOT/DSCs and iodide/DSCs was measured with an impedance analyzer (Solartron Analytical, 1260) connected with a potentiostat (Solartron Analytical, 1287) under air mass 1.5 (100 mW cm^{-2}) conditions at 25 °C. The EIS was recorded over a frequency range of 1−10^6 Hz. The ac amplitude and the applied voltage were 10 mV and set at V_{oc} of the cells, respectively. The interfacial charge-transfer resistances and the electrochemical capacitances formed between interfaces were analyzed using the Z-View software (Solarton Analytical).

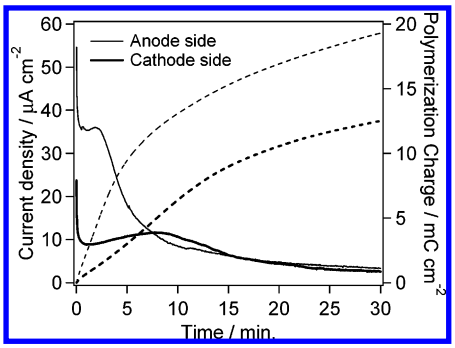

Figure 4. Chronoamperogram (solid curves) and total polymerization charge (dotted curves) on the dyed TiO_2 film polymerized by anode-side irradiation (thin curves) and cathode-side irradiation (bold curves).

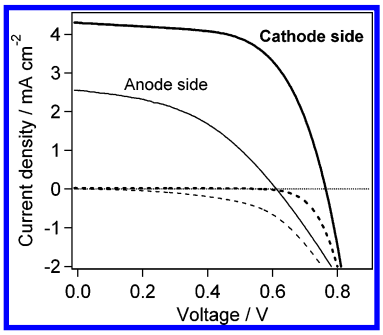

Figure 5. Photocurrent−voltage characteristic for PEDOT/DSCs fabricated by cathode-side illumination (bold curve) and anode-side illumination (solid curve) under AM1.5 irradiation and their dark currents (dotted curves). The best performances of the cells are chosen.

Results

Polymerization of PEDOT and Photocurrent−Voltage Characteristics for PEDOT/DSCs. The total polymerization charge of PEDOT in dyed TiO_2 layers (ca. 5 μm thick) obtained from potentiostatic polymerization for 30 min, J_{sc}, V_{oc}, FF, and the resulting η of PEDOT/DSCs are listed in Table 1. These samples shown here are the ones fabricated using $LiClO_4$ during in-situ photo-electrochemical polymerization. The "anode side" and "cathode side'" mean the direction of Xe lamp illumination during PEDOT/DSCs fabrication as shown in Figure 3. Figure 4 shows the polymerization current and polymerization charge obtained for in-situ photo-electrochemical polymerization of bis-EDOT by anode-side or cathode-side illumination under potentiostatic condition. Figure 5 and Figure 6 show the photocurrent−voltage characteristics and IPCE spectra for PEDOT/DSCs fabricated by the different directions of illumination under air mass 1.5 (100 mW cm^{-2}) conditions at 25 °C. IPCE of the cathode-side illuminated cell was more than 0.3 at 480−520 nm. The average performance of the cells fabricated by cathode-side illumination were J_{sc} = 3.20 mA cm^{-2}, V_{oc} = 0.77 V, FF = 0.50, and η = 1.25%, respectively.

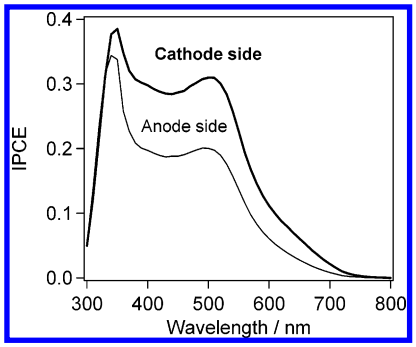

Figure 6. IPCE spectra of PEDOT/DSCs fabricated by cathode-side illumination (bold curve) and anode-side illumination (solid curve).

TABLE 2: Polymerization Charges of PEDOT in Mesopores of TiO_2 Layers and the Cell Performance of PEDOT/DSCs and Iodide/DSCs, Which Were Used in Electron Diffusion Coefficients and Electron Lifetime Measurements

type-thickness (μm)	polymerization charge (mC cm^{-2})	J_{sc} (mA cm^{-2})	V_{oc} (V)	FF	η (%)
PEDOT-2.5	9.4	2.60	0.67	0.47	0.81
PEDOT-2.0	11.0	2.70	0.77	0.67	1.39
PEDOT-2.6	11.0	2.81	0.79	0.67	1.49
PEDOT-2.6	13.2	3.06	0.60	0.60	1.11
iodide-2.5		9.84	0.72	0.69	4.91

In addition, the dark current of the cell fabricated by cathode-side illumination was improved compared to that obtained by anode-side illumination. Both the photocurrent−voltage characteristics and IPCE spectrum of the cell fabricated by cathode-side illumination showed higher values in all parameters except the total polymerization charge compared to the cell fabricated by anode-side illumination. Further fabrication of PEDOT/DSCs was worked out by cathode-side illumination.

Electron Diffusion Coefficients in Mesoporous TiO_2 Electrodes of Both PEDOT/DSCs and Iodide/DSCs. The electron diffusion coefficient was estimated by the following equation.[45] $D = w^2/2.35\tau_c$, where w is the thickness of the TiO_2 layer and τ_c is the time constant, which was obtained by fitting the transient photocurrent decay with $\exp(-t/\tau_c)$. The samples of both PEDOT/DSCs (fabricated using $LiClO_4$) and iodide/DSCs with ca. 2.5 μm TiO_2 thickness were used in the electron diffusion coefficient measurements in order to minimize the influence of electron recombination with dye cations or holes inside PEDOT on the presupposition of this measurement. The performance of PEDOT/DSCs and iodide/DSCs used in the measurements was $\eta = 0.8-1.5$ and 4.9%, respectively (Table 2). The polymerization charges of PEDOT in mesoporous dyed TiO_2 layers were changed from 9 to 13 mC cm^{-2} by controlling the polymerization time from 15 to 30 min. Figure 7 shows the transient photocurrent decay of both PEDOT/DSCs and iodide/DSCs at near J_{sc} value (PEDOT, 0.38 mA cm^{-2}; liquid, 0.45 mA cm^{-2}, respectively) under the diode laser irradiation. The transient photocurrent decay of PEDOT/DSCs was faster than that of iodide/DSCs in the same time range. Figure 8 shows the estimated electron diffusion coefficients by the above equation in the mesoporous TiO_2 electrodes of both of PEDOT/DSCs with different polymerization charge (9−13 mC cm^{-2}) and iodide/DSCs as a function of J_{sc}. The several samples of PEDOT/DSCs and iodide/DSCs were used in this measurement. The plotted triangles in Figure 8 show PEDOT/DSCs, and squares show iodide/DSCs. The photocurrent J_{sc} of almost all samples was assumed proportional to the intensity of the laser. From both Figure 7 and Figure 8, the estimated diffusion

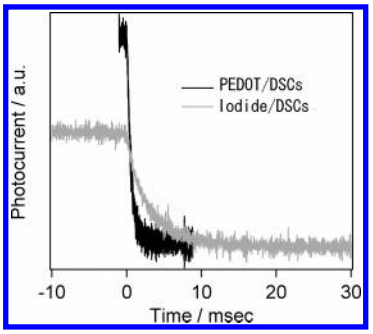

Figure 7. Transient photocurrent decay of both PEDOT/DSCs and iodide/DSCs at nearly the same J_{sc} (PEDOT/DSCs, 0.38 mA/cm^2; iodide/DSCs, 0.45 mA/cm^2, respectively) under diode laser irradiation.

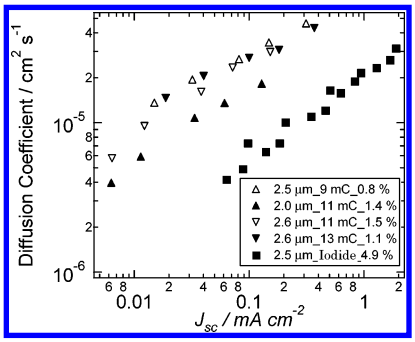

Figure 8. Electron diffusion coefficients in TiO_2 electrode of PEDOT/DSCs (triangles) or iodide/DSCs (squares) as a function of J_{sc}. Insert shows the thickness of the TiO_2 layer, the polymerization charge of PEDOT, and the energy conversion efficiency η at AM1.5 irradiation. All samples show the power law dependence on J_{sc}.

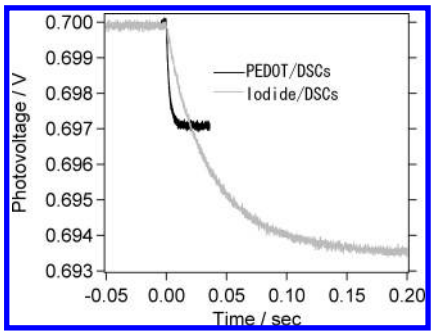

Figure 9. Transient photovoltage decay of both PEDOT/DSCs and iodide/DSCs at nearly the same J_{sc} (PEDOT/DSCs, 0.38 mA/cm^2; iodide/DSCs, 0.45 mA/cm^2, respectively) under diode laser irradiation.

coefficient of PEDOT/DSCs was 2−3 times higher than that of iodide/DSCs.

Electron Lifetimes in TiO_2 Electrodes of Both PEDOT/DSCs and Iodide/DSCs. For electron lifetime measurements, the same samples as for the electron diffusion coefficient measurements were used. The electron lifetimes in TiO_2 electrodes of both PEDOT/DSCs and iodide/DSCs were obtained from SLIM-PCV measurements by fitting photovoltage decay with $\exp(-t/\tau)$.[45] Figure 9 shows the transient photovoltage decay of both PEDOT/DSCs and iodide/DSCs at near J_{sc} value (PEDOT, 0.38 mA cm^{-2}; liquid, 0.45 mA cm^{-2}, respectively) under diode laser irradiation. The photovoltage decay of PEDOT/DSCs was faster and ca. 4 mV smaller than that of iodide/DSCs in the same time range. Figure 10 shows electron lifetimes in TiO_2 electrodes determined for both PEDOT/DSCs with different polymerization charge (9−13 mC cm^{-2}) and iodide/DSCs as a function of J_{sc}. From both Figure 9 and Figure 10, the electron lifetime of PEDOT/DSCs was 10−30 times shorter than that of iodide/DSCs. Figure 11 shows

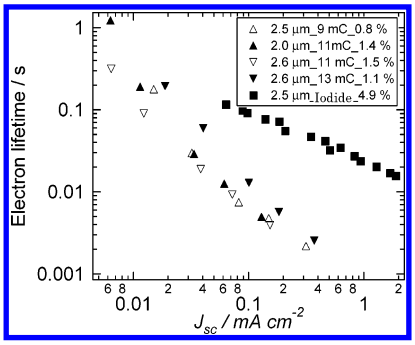

Figure 10. Electron lifetimes in the TiO_2 electrode of PEDOT/DSCs (triangles) and iodide/DSCs (squares) under open-circuit conditions as a function of J_{sc}. Insert shows the thickness of the TiO_2 layer, the polymerization charge of PEDOT, and energy conversion efficiency η at AM1.5 irradiation.

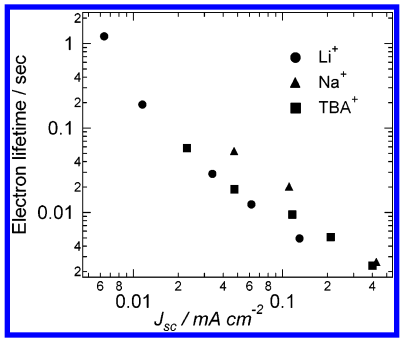

Figure 11. Electron lifetimes in the TiO_2 electrode of PEDOT/DSCs fabricated by using different cations, Li (circles), Na (triangles), and TBA (squares), during polymerization under open-circuit conditions as a function of J_{sc}. All samples contain $EMIm^+$ cations as a solid-state electrolyte.

TABLE 3: Polymerization Charge and the Cell Performance of PEDOT/DSCs Containing Different Cation in in-situ Photoelectrochemical Polymerization of Bis-EDOT

	polymerization charge (mC cm^{-2})	J_{sc} (mA cm^{-2})	V_{oc} (V)	FF	η (%)
Li^+ [a]	11.2 ± 0.2	2.85 ± 0.09	0.78 ± 0.02	0.65 ± 0.06	1.42 ± 0.10
Na^+ [a]	14.1 ± 0.4	3.54 ± 0.37	0.59 ± 0.10	0.52 ± 0.09	1.07 ± 0.26
TBA^+ [b]	10.9 ± 0.5	2.96 ± 0.30	0.53 ± 0.03	0.43 ± 0.01	0.67 ± 0.03

[a] Average of 4 samples. [b] Average of 3 samples.

the electron lifetimes of PEDOT/DSCs fabricated using in-situ photo-electrochemical polymerization in the presence of different cations, Li^+, Na^+, or TBA^+, as the counterion of ClO_4^- as a dopant. All samples contain $EMIm^+$ cation that comes from the added ionic liquid to enhance electron diffusion in mesoporous TiO_2 layer. The η of the cells used in the measurement was 0.7−1.4%, as shown in Table 3. The electron lifetime of these samples was almost the same.

EIS Measurements of Both PEDOT/DSCs and Iodide/DSCs. The performances of PEDOT/DSCs and iodide/DSCs used in EIS measurements were $\eta = 1.2$ and 4.8%, respectively. Figure 12 shows the Cole−Cole plot of both PEDOT/DSCs and iodide/DSCs under open-circuit conditions. The insert shows the magnified Cole−Cole plot of iodide/DSCs. Figure 13 shows the magnified Cole−Cole plot of PEDOT/DSCs in the frequency range from 2.5×10^5 to 1.6×10^3 Hz. The Z_{real} and $-Z_{image}$ was the real part and imaginary part of the impedance, corresponding to the charge-transfer resistance formed between interfaces and the resistance formed by the existence of electrochemical capacitance, respectively. In both DSCs, two semicircles were observed and the total impedance of PEDOT/

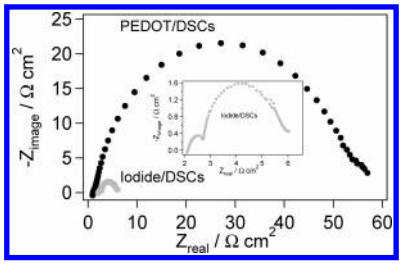

Figure 12. Impedance spectra of PETOT/DSCs (triangles) and iodide/DSCs (squares) obtained under AM1.5 irradiation. Insert is the magnified spectrum of iodide/DSCs.

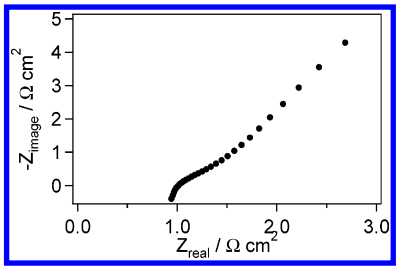

Figure 13. Impedance spectrum of PEDOT/DSCs magnified in the high-frequency region from 2.5×10^5 to 1.6×10^3 Hz obtained under AM1.5 irradiation.

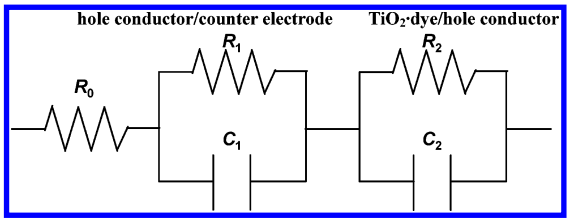

Figure 14. Equivalent circuit supposed from Cole−Cole plot of PEDOT/DSCs and iodide/DSCs.

DSCs was higher than that of iodide/DSCs. In the case of PEDOT/DSCs, the small semicircle in the frequency range from 2.5×10^5 to 2.0×10^4 Hz in Figure 13 and the big one in the frequency range from 2.5×10^3 to 2.0×10 Hz in Figure 12 were observed. In the case of iodide/DSCs, two semicircles, the first one in the frequency range from about 10^5 to 3.0×10^3 Hz and the second one in the frequency range from about 10^3 to 2.0×10 Hz, were observed in the inset of Figure 12. These semicircles are attributed to the impedance related to Pt/electrolyte containing the I^-/I_3^- interface and TiO_2/dye/electrolyte containing the I^-/I_3^- interface, respectively.[44] On the basis of impedance analysis of iodide/DSCs, we assumed that the frequency dependence of the impedance on the specific interfaces of iodide/DSCs, such as TiO_2/dye/electrolyte, corresponds to those interfaces of PEDOT/DSCs such as TiO_2/dye/PEDOT. Considering this hypotheses, the equivalent circuits of DSCs which contain two *RC* parallel circuits[42,44] can be proposed at least in the above frequency region as shown in Figure 14. *R* and *C* were used for fitting the impedance spectra obtained for both cells with Z-view software. R_1C_1 and R_2C_2 describe a charge-transfer resistance and an electrochemical capacitance formed by counter electrode/hole transport layer interface and TiO_2/dye/hole transport layer interface, respectively on the basis of the above hypotheses. R_0 describes the sheet resistance of DSCs.[42−44] Those values of *R* and *C* obtained by fitting were shown in Table 4. Comparing the values obtained for both cells indicated that PEDOT/DSCs exhibited a higher value for R_1 and R_2 charge-transfer resistances and a lower value for C_1 and C_2 electrochemical capacitances than iodide/DSCs.

TABLE 4: Parameters Obtained by Fitting the Impedance Spectra of PEDOT/DSCs and Iodide/DSCs Shown in Figure 12 Using the Equivalent Circuit

	R_0 (Ω cm^2)	R_1 (Ω cm^2)	C_1 (F cm^{-2})	R_2 (Ω cm^2)	C_2 (F cm^{-2})
PEDOT/DSCs	1.02	3.13	1.73×10^{-5}	52.6	3.04×10^{-5}
iodide/DSCs	2.33	0.76	3.70×10^{-5}	3.27	1.22×10^{-3}

Discussions

Polymerization of PEDOT and Photocurrent−Voltage Characteristics for PEDOT/DSCs. Although the total polymerization charge of PEDOT in the cathode-side illumination was smaller than that in anode-side illumination (Figure 4), the cell performances of the former one were better than those of the latter one as shown in Table 1. By the cathode-side illumination of the Xe lamp, it seems that PEDOT is easier to polymerize at the cathode side of the dyed TiO_2 film than at the FTO side. The enhancement of J_{sc} seems to be attributed to the improvement of electric contact between some dye molecules, the hole conductor, PEDOT, and Au counter electrode, resulting in the smooth unidirectional electron transfer from Au electrode to PEDOT and some dye molecules. In addition, the short-circuiting between PEDOT and FTO glass substrates due to the direct contact between them has hardly occurred in the case of cathode-side illumination than in the case of anode-side illumination. Both the enhancement of V_{oc} and FF and the reduction of dark current in cathode-side illumination indicate that the back-electron transfer and the electron leakage from both the conduction band of TiO_2 and FTO to PEDOT should be suppressed. In other words, the enhancement of shunt resistance and the reduction of series resistance of the PEDOT/DSCs can be rationalized due to unidirectional electron flow at the interfaces. It was found that the cathode-side illumination method in polymerization of PEDOT into the mesopores of the dyed TiO_2 layer led to rectifiable improvement of PEDOT/DSCs. As shown in Figure 6, the calculated J_{sc} from IPCE spectrum of PEDOT/DSCs made by the cathode-side illumination is approximately 60% higher than that of the anode-side illumination, which is agree with the increase of J_{sc} from 2.6 to 4.3 mA cm^{-2} observed in Figure 5. The molecular distribution control of PEDOT in TiO_2 electrodes will be very significant for achieving high η of PEDOT/DSCs.

Electron Diffusion Coefficients in TiO_2 Electrodes of Both PEDOT/DSCs and Iodide/DSCs. The electron diffusion coefficient of PEDOT/DSCs was found higher than that of iodide/DSCs. The TiO_2 layers in both PEDOT/DSCs and iodide/DSCs adsorbed not only dye molecules but also Li^+ and alkylimidazolium ($EMIm^+$ or $DMPIm^+$) cations from electrolytes. The strong adsorption of them on the TiO_2 surface leads to the promotion of electron diffusion in TiO_2 electrodes, which is rationalized as ambipolar diffusion.[10,34,35] The ambipolar diffusion plays an important role in the electron diffusion coefficients in PEDOT/DSCs because of the addition of ionic liquid $EMIm^+$. In addition, we assume that many radical cations existing in PEDOT[22,23] probably influence on ambipolar diffusion in TiO_2 layer of PEDOT/DSCs. In other words, Coulomb force of the PEDOT which is in the form of radical cations may lead to activation of the electron/hole dynamics and promote the ambipolar diffusion in TiO_2 anodes, resulting in higher electron diffusion coefficient compared to that in iodide/DSCs.

Electron Lifetime in TiO_2 Electrodes of Both PEDOT/DSCs and Iodide/DSCs. In Figure 9, the photovoltage decay range of PEDOT/DSCs was ca. 4 mV smaller than that of iodide/DSCs. The electron lifetime in TiO_2 electrodes of PEDOT/DSCs was determined 10−30 times shorter than that of iodide/DSCs as shown in Figure 10. In iodide/DSCs, the electron recombination in TiO_2 electrodes occurs with either dye cations or I_3^- in the liquid electrolyte. Several researchers have observed that the electron recombination from TiO_2 to dye cations occurs in microsecond to millisecond order in open-circuit conditions and the electron transfer from I^- to dye cations occurs in ~100 ns in the literatures.[5,9,37,47] Therefore, the electron recombination in TiO_2 electrodes may occur mainly with I_3^- rather than with the oxidized dye cations. The electron lifetime of iodide/DSCs in Figure 10 means that solvent molecules in mesoporous TiO_2 layer of iodide/DSCs may suppress the back-electron transfer to I_3^- [45] to some extent, which results in longer electron lifetime compared to that of PEDOT/DSCs. In PEDOT/DSCs, the electrons in TiO_2 electrodes recombine with either dye cations or holes in PEDOT as in the case of I_3^- in iodide/DSCs. The recombination with dye cations may prevail if occur because the amount of the PEDOT formed in the vicinity of dye molecules could not be large in this case as discussed later. However, nobody has yet investigated which electron recombination process is dominant. The high conductivity of PEDOT in the mesopores of the dyed TiO_2 layer results in effective charge migrating from PEDOT to Au counter electrode. The number of hole carriers compensated by ClO_4^- in PEDOT affects on the conductivity of PEDOT, giving good influences on unidirectional electron flow in PEDOT/DSCs. The amount of PEDOT molecules depends on the polymerization charge. On the other hand, Figure 10 shows that the electron lifetimes of the DSCs fabricated with 9−13 mC cm^{-2} were nearly the same. This indicates that the electron lifetime of PEDOT/DSCs was hardly affected by the polymerization charge of PEDOT in the examined range. As shown in Figure 11, the electron lifetime of PEDOT/DSCs was independent of the cationic species used in polymerization. These results indicate that the electron lifetime in TiO_2 electrodes of PEDOT/DSCs is affected by $EMIm^+$ cations rather than by the other cations used in the polymerization because the $EMIm^+$ cations are adsorbed strongly on the TiO_2 layer,[35] resulting in the suppression of back-electron transfer from TiO_2 to oxidized dye or PEDOT.[25]

EIS Measurement of Both PEDOT/DSCs and Iodide/DSCs. Since both the frequency dependence and the size of the semicircle of the EIS measurements of the Pt/electrolyte/Pt cell was similar to that reported by Han et al.,[44] we assumed the two semicircles appeared in the Cole−Cole plot of iodide/DSCs (the inset of Figure 12) were assigned to the impedance related to Pt/electrolyte interface and TiO_2/dye/electrolyte interface, respectively. PEDOT/DSCs showed two semicircles in Figure 12 and Figure 13, the same as the case of iodide/DSCs. The first semicircle in the higher frequency region can be explained by the impedance related to Au/PEDOT interface, and the second one in the lower frequency region can be attributed to TiO_2·dye/PEDOT interface by regarding the interfaces with electrolyte in iodide/DSCs as those with PEDOT. The difference in frequency dependence between Au/PEDOT and Pt/electrolyte interfaces may be explained as due to utilization of different materials both as the counter electrode and the hole transport layer.

Considering the equivalent DSCs circuits which contain two *RC* parallel circuits formed by counter electrode/hole transport layer interface and TiO_2·dye/hole transport layer interface[42−44] at least in the above frequency region, sheet resistance R_0, charge-transfer resistances R_1 and R_2, and electrochemical capacitances C_1 and C_2 were evaluated as listed in Table 4.

Comparing the values obtained for both cells, PEDOT/DSCs exhibited a higher value for R_1 and R_2 charge-transfer resistances and lower value for C_1 and C_2 electrochemical capacitances than those of iodide/DSCs. Such differences indicate the different size in the area of electric contact between the TiO_2/dye and the hole transport PEDOT layer. Especially, the values of R_2 and C_2 corresponding to the TiO_2/dye/hole transport layer interface were greatly different between PEDOT/DSCs and iodide/DSCs. This clearly indicates poorer electric contact between TiO_2/dye and PEDOT than that between the TiO_2/dye and the liquid electrolyte, resulting in higher R_2 and lower C_2.

Strategy for Further Improvement of PEDOT/DSCs. The comparison of electron transport property can be done by comparing diffusion length (L) of electrons, which is given by the square root of the multiplication of diffusion coefficient and lifetime. For example, L of PEDOT/DSCs and iodide/DSCs under the irradiation giving $J_{sc} = 0.1$ mA/cm^2 were ca. 5 and 7 μm, respectively. The L under AM 1.5 irradiation are smaller than those values since L is somehow compensated by an increase of light intensity. This implies that the thickness of the TiO_2 layer of PEDOT/DSCs with maximum η, i.e., 5 μm, is appropriate because the value is comparable to the determined L value.

The dominant problem of the smaller L in PEDOT/DSCs is the shorter lifetime of electrons caused by recombination processes. As for the distribution of PEDOT, the volume and the average chain length of the formed PEDOT can be roughly calculated from the polymerization charge, the density of PEDOT (1.34 g cm^{-3}), and the porosity of TiO_2 layer (0.53 for the films made of Nanoxide-T). For example, the ratio of the volume occupied with PEDOT in mesoporous TiO_2 was given ca. 20%, and the average chain length based on homogeneous polymerization from each dye molecule was ca. 6.8 EDOT units under the conditions of the polymerization charge of 25 mC cm^{-2} and the TiO_2 thickness of 5 μm. Taking these into consideration, the electron recombination in the TiO_2 layer of PEDOT/DSCs should occur mainly with dye cations rather than with radical cations from PEDOT. That is, the large number of dye cations could not be reduced because the dye molecules connected appropriately with PEDOT, which is polymerized inhomogeneously in the TiO_2 layer, is supposed to be small in quantity which is in agreement with quite values of the low capacitance C_2 and the high resistance R_2. The insufficient connection between the Z-907 molecules and PEDOT also causes the lower FF of PEDO/DSCs. The novel approach to construct the efficient interface can be done by employing new ruthenium dye.[48]

Through the above discussions, it was confirmed that the lower photovoltaic performance of PEDOT/DSCs was rationalized as due to the shorter electron lifetime and the higher resistances (lower capacitances) than those in iodide/DSCs. From these viewpoints, it was clearly suggested that the mesopores of the TiO_2 layer should be fully charged with PEDOT, which should maximize the electric contact between the dye molecules and the hole conducting materials, PEDOT, in dye photovoltaics.

Conclusions

The performance of PEDOT/DSCs was improved when Xe lamp illumination was performed from the cathode side during in-situ photo-electrochemical polymerization of PEDOT, resulting in $J_{sc} = 4.3$ mA cm^{-2}, $V_{oc} = 0.76$ V, FF $= 0.64$, and $\eta = 2.1\%$, respectively, under air mass 1.5 condition. The electric contact between PEDOT and Au counter electrode was improved by the cathode-side illumination of the Xe lump. Furthermore, the electron transport processes in PEDOT/DSCs analyzed by the SLIM-PCV measurements and the EIS measurements in comparison with those in iodide/DSCs suggests the importance of constructing the interfaces that in the PEDOT/DSCs, namely, the interface molecular organization should be optimized for concurrent increase of V_{oc}, J_{sc}, and FF. The key issue of PEDOT/DSCs is the polymerization in mesoscopic TiO_2 anodes, i.e., dense introduction of conductive PEDOT molecules with controlled interface structure.

Acknowledgment. This work was partially supported by Grant-in-Aid for the Creation of Innovations through Business-Academic-Public Sector Cooperation, Open Competition for the Development of Innovative Technology (Grant No. 12310) from the Ministry of Education, Culture, Sports, Science and Technology of Japan, and by the Strategic Research Base, Frontier Research Center (Graduate School of Engineering), Osaka University, from the Japan Government's Special Coordination Fund for Promoting Science and Technology. We thank Bayer AG for the supply of 3,4-ethylenedioxythiophene. We also give special thanks to Dr. Shogo Nakade for the guidance of SLIM-PCV measurements.

Supporting Information Available: Schematic description of the structure of PEDOT/DSC (S1) and the surface scanning electron microscopy photograph of the TiO_2 anode after polymerization of PEDOT under cathode-side illumination (S2). This material is available free of charge via the Internet at http://pubs.acs.org.

References and Notes

(1) O'Regan, B.; Grätzel, M. *Nature (London)* **1991**, *353*, 737.
(2) Nazeeruddin, M. K.; Kay, A.; Rodicio, I.; Humphry-Baker, R.; Müeller, E.; Liska, P.; Vlachopoulos, N.; Grätzel, M. *J. Am. Chem. Soc.* **1993**, *115*, 6382.
(3) Hagfeldt, A.; Grätzel, M. *Acc. Chem. Res.* **2000**, *33*, 269.
(4) Nazeeruddin, M. K.; Angelis, F. D.; Fantacci, S.; Selloni, A.; Viscardi, G.; Liska, P.; Ito, S.; Bessho, T.; Grätzel, M. *J. Am. Chem. Soc.* **2005**, *127*, 16835.
(5) Tachibana, Y.; Moser, J. E.; Grätzel, M.; Klug, D. R.; Durrant, J. R. *J. Phys. Chem.* **1996**, *100*, 20056.
(6) Solbrand, A.; Lindström, H.; Rensmo, H.; Hagfeldt, A.; Lindquist, S. E.; Södergren, S. *J. Phys. Chem. B* **1997**, *101*, 2514.
(7) Nazeeruddin, M. K.; Péchy, P.; Renouard, T.; Zakeeruddin, S. M.; Humphry-Baker, R.; Comte, P.; Liska, P.; Cevey, L.; Costa, E.; Shklover, V.; Spiccia, L.; Deacon, G. B.; Bignozzi, C. A.; Grätzel, M. *J. Am. Chem. Soc.* **2001**, *123*, 1613.
(8) Kay, A.; Grätzel, M. *Sol. Energy Mater. Sol. Cells* **1996**, *44*, 99.
(9) Wang, P.; Zakeeruddin, S. M.; Moser, J. E.; Nazeeruddin, M. K.; Sekiguchi, T.; Grätzel, M. *Nat. Mater.* **2003**, *2*, 402.
(10) Kubo, W.; Kambe, S.; Nakade, S.; Kitamura, T.; Hanabusa, K.; Wada, Y.; Yanagida, S. *J. Phys. Chem. B* **2003**, *107*, 4374.
(11) Mohmeyer, N.; Wang, P.; Schmidt, H.-W.; Zakeeruddin, S. M.; Grätzel, M. *J. Mater. Chem.* **2004**, *14*, 1905.
(12) Nogueira, A. F.; Paoli, M. A. D.; Montanari, I.; Monkhouse, R.; Nelson, J.; Durrant, J. R. *J. Phys. Chem. B* **2001**, *105*, 7517.
(13) Tennakone, K.; Kumara, G. R. R. A.; Kottegoda, I. R. M.; Wijayantha, K. G. U.; Perera, V. P. S. *J. Phys. D: Appl. Phys.* **1998**, *31*, 1492.
(14) O'Regan, B.; Schwartz, D. T.; Zakeeruddin, S. M.; Grätzel, M. *Adv. Mater.* **2000**, *12*, 1263.
(15) O'Regan, B.; Lenzmann, F. *J. Phys. Chem. B* **2004**, *108*, 4342.
(16) Kitamura, T.; Maitani, M.; Matsuda, M.; Wada, Y.; Yanagida, S. *Chem. Lett.* **2001**, *1054*.
(17) Bach, U.; Lupo, D.; Comte, P.; Moser, J. E.; Weissörtel, F.; Salbeck, J.; Spreitzer, H.; Grätzel, M. *Nature (London)* **1998**, *395*, 583.
(18) Krüger, J.; Plass, R.; Grätzel, M.; Matthieu, H. J. *Appl. Phys. Lett.* **2002**, *81*, 367.
(19) Scmit-Mende, L.; Bach, U.; Humphry-Baker, R.; Horiuchi, T.; Miura, H.; Ito, S.; Uchida, S.; Grätzel, M. *Adv. Mater.* **2005**, *17*, 813.
(20) Groenendaal, L. B.; Jonas, F.; Freitag, D.; Pielartzik H.; Reynolds, J. R. *Adv. Mater.* **2000**, *12*, 481.

(21) Groenendaal, L. B.; Zotti, G.; Aubert, P.-H.; Waybright, S. M.; Reynolds, J. R. *Adv. Mater.* **2003**, *15*, 855.
(22) Lu, W.; Fadeev, A. G.; Qi, B.; Smela, E.; Mattes, B. R.; Ding, J.; Spinks, G. M.; Mazurkiewicz, J.; Zhou, D.; Wallace, G. G.; MacFarlane, D. R.; Forsyth, S. A.; Forsyth, M. *Science (Washington, D. C.)* **2002**, *297*, 5583.
(23) Ha, Y.-H.; Nikolov, N.; Pollack, S. K.; Matsrangelo, J.; Martin, B. D.; Shashidhar, R. *Adv. Funct. Mater.* **2004**, *14*, 615.
(24) Saito, Y.; Kitamura, T.; Wada, Y.; Yanagida, S. *Chem. Lett.* **2002**, 1060.
(25) Saito, Y.; Kitamura, T.; Wada, Y.; Yanagida, S. *Synth. Met.* **2002**, *131*, 185.
(26) Saito, Y.; Fukuri, N.; Senadeera, G. K. R.; Kitamura, T.; Wada, Y.; Yanagida, S. *Electrochem. Commun.* **2004**, *6*, 71.
(27) Fukuri, N.; Saito, Y.; Kubo, W.; Senadeera, G. K. R.; Kitamura, T.; Wada, Y.; Yanagida, S. *J. Electrochem. Soc.* **2004**, *151*, A1745.
(28) Dloczik, L.; Ileperuma, O.; Lauermann, I.; Peter, L. M.; Ponomarev, E. A.; Redmond, G.; Shaw, N. J.; Uhlendorf, I. *J. Phys. Chem. B* **1997**, *101*, 10281.
(29) Franco, G.; Peter, L. M.; Ponomarev, E. A. *Electrochem. Commun.* **1999**, *1*, 61.
(30) Lagemaat, J. v. d.; Park, N.-G.; Frank, A. J. *J. Phys. Chem. B* **2000**, *104*, 2044.
(31) Nakade, S.; Kubo, W.; Saito, Y.; Kanzaki, T.; Kitamura, T.; Wada, Y.; Yanagida, S. *J. Phys. Chem. B* **2003**, *107*, 14244.
(32) Schlichthörl, G.; Huang, S. Y.; Sprague, J.; Frank, A. J. *J. Phys. Chem. B* **1997**, *101*, 8141.
(33) Zaban, A.; Greenshtein, M.; Bisquert, J. *Chem. Phys. Chem.* **2003**, *4*, 859.
(34) Nakade, S.; Kambe, S.; Kitamura, T.; Wada, Y.; Yanagida, S. *J. Phys. Chem. B* **2001**, *105*, 9150.
(35) Kambe, S.; Nakade, S.; Kitamura, T.; Wada, Y.; Yanagida, S. *J. Phys. Chem. B* **2002**, *106*, 2967.
(36) Huang, S. Y.; Schlichthöl, G.; Nozik, A. J.; Grätzel, M.; Frank, A. J. *J. Phys. Chem. B* **1997**, *101*, 2576.
(37) Haque, S. A.; Tachibana, Y.; Willis, R. L.; Moser, J. E.; Grätzel, M.; Klug, D. R.; Durrant, J. R. *J. Phys. Chem. B* **2000**, *104*, 538.
(38) Nakade, S.; Kanzaki, T.; Kubo, W.; Kitamura, T.; Wada, Y.; Yanagida, S. *J. Phys. Chem. B* **2005**, *109*, 3480.
(39) Krüger, J.; Plass, R.; Grätzel, M.; Cameron, P. J.; Peter, L. M. *J. Phys. Chem. B* **2003**, *107*, 7536.
(40) Hauch, A.; George, A. *Electrochim. Acta* **2001**, *46*, 3457.
(41) Kern, R.; Sastrawan, R.; Ferber, J.; Stangl, R.; Luther, J. *Electrochim. Acta* **2002**, *47*, 4213.
(42) Longo, C.; Nogueira, A. F.; Paoli, M.-A. D. *J. Phys. Chem. B* **2002**, *106*, 5925.
(43) Kron, G.; Egerter, T.; Werner, J. H.; Rau, U. *J. Phys. Chem. B* **2003**, *107*, 3556.
(44) Han, L.; Koide, N.; Chiba, Y.; Mitate, T. *Appl. Phys. Lett.* **2004**, *84*, 2433.
(45) Nakade, S.; Kanzaki, T.; Wada, Y.; Yanagida, S. *Langmuir* **2005**, *21*, 10803.
(46) Sotzing, G. A.; Reynolds, J. R.; Steel, P. J. *Adv. Mater.* **1997**, *9*, 795.
(47) Haque, S. A.; Tachibana, Y.; Klug, D. R.; Durrant, J. R. *J. Phys. Chem. B* **1998**, *102*, 1745.
(48) Mozer, A. J.; Jiang, K. J.; Wada, Y.; Masaki, N.; Mori, S. N.; Yanagida, S. *Appl. Phys. Lett.* **2006**, *89*, 043509.